Title page

- **The name(s) of the author(s)**

  Yusuke Imanaka

- **A concise and informative title**

  Inherited CARD9 deficiency in a child with invasive disease due to *Exophiala dermatitidis* and two older but asymptomatic siblings

- **The affiliation(s) and address(es) of the author(s)**

・Yusuke Imanaka
Department of Pediatrics, Hiroshima University Graduate School of Biomedical and Health Science, Hiroshima, Japan
lowiqyou@yahoo.co.jp

・Maki Taniguchi
Department of Pediatrics, Hiroshima University Graduate School of Biomedical and Health Science, Hiroshima, Japan
taniguchi-mk@hiroshima-u.ac.jp

・Takehiko Doi
Department of Pediatrics, Hiroshima University Graduate School of Biomedical and Health Science, Hiroshima, Japan
take-doi02@hiroshima-u.ac.jp

・Miyuki Tsumura
Department of Pediatrics, Hiroshima University Graduate School of Biomedical and Health Science, Hiroshima, Japan
m055@hiroshima-u.ac.jp

・Rie Nagaoka
Division of Infectious Diseases Laboratory Medicine, Hiroshima University Hospital, Hiroshima, Japan
pmarie@hiroshima-u.ac.jp

・Maiko Shimomura

Department of Pediatrics, Hiroshima University Graduate School of Biomedical and Health Science, Hiroshima, Japan
shimomai0105@hiroshima-u.ac.jp

・Takaki Asano
Department of Pediatrics, Hiroshima University Graduate School of Biomedical and Health Science, Hiroshima, Japan
St. Giles Laboratory of Human Genetics of Infectious Diseases, Rockefeller Branch, Rockefeller
tasano@rockefeller.edu

・Reiko Kagawa
Department of Pediatrics, Hiroshima University Graduate School of Biomedical and Health Science, Hiroshima, Japan
ykagawa@ja2.so-net.ne.jp

・Yoko Mizoguchi
Department of Pediatrics, Hiroshima University Graduate School of Biomedical and Health Science, Hiroshima, Japan
ymizoguchi@gmail.com

・Shuhei Karakawa
Department of Pediatrics, Hiroshima University Graduate School of Biomedical and Health Science, Hiroshima, Japan
kara1224@hiroshima-u.ac.jp

・Koji Arihiro
Department of Anatomical Pathology, Hiroshima University Hospital, Hiroshima, Japan
arihiro@hiroshima-u.ac.jp

・Kohsuke Imai
Department of Pediatrics and Developmental Biology, Graduate School of Medical and Dental Sciences, Tokyo Medical and Dental University, Tokyo, Japan
kimai.ped@tmd.ac.jp

・Tomohiro Morio

Department of Pediatrics and Developmental Biology, Graduate School of Medical and Dental Sciences, Tokyo Medical and Dental University, Tokyo, Japan
tmorio.ped@tmd.ac.jp

・Jean-Laurent Casanova
St. Giles Laboratory of Human Genetics of Infectious Diseases, Rockefeller Branch, Rockefeller University, New York, NY, United States
Laboratory of Human Genetics of Infectious Diseases, Necker Branch, INSERM UMR 1163, Imagine Institute, Paris, France
University of Paris, Paris, France, EU
Howard Hughes Medical Institute, New York, USA
casanova@rockefeller.edu

・Anne Puel
St. Giles Laboratory of Human Genetics of Infectious Diseases, Rockefeller Branch, Rockefeller University, New York, NY, United States
Laboratory of Human Genetics of Infectious Diseases, Necker Branch, INSERM UMR 1163, Imagine Institute, Paris, France
University of Paris, Paris, France, EU
anne.puel@inserm.fr

・Osamu Ohara
Department of Applied Genomics, Kazusa DNA Research Institute, Kisarazu, Japan
ohara@kazusa.or.jp

・Katsuhiko Kamei
Department of Medical Mycology Research Center, Chiba University, Japan
kkamei-chiba@umin.ac.jp

・Masao Kobayashi
Department of Pediatrics, Hiroshima University Graduate School of Biomedical and Health Science, Hiroshima, Japan
Japan Red Cross, Chugoku-Shikoku Block Blood Center, Hiroshima, Japan
masak@hiroshima-u.ac.jp

・Satoshi Okada

Department of Pediatrics, Hiroshima University Graduate School of Biomedical and Health Science, Hiroshima, Japan
sokada@hiroshima-u.ac.jp

- **The e-mail address, telephone and fax numbers of the corresponding author**

Correspondence to Satoshi Okada
Department of Pediatrics, Hiroshima University Graduate School of Biomedical and Health Sciences
1-2-3 Kasumi, Minami-Ku, Hiroshima-Shi, Hiroshima, 734-8551, Japan
E-mail: sokada@hiroshima-u.ac.jp
Tell: +81-82-257-5212
Fax: +81-82-257-5214

120 **Inherited CARD9 deficiency in a child with invasive disease due to *Exophiala dermatitidis* and two**

121 **older but asymptomatic siblings**

122

123 **Authors**

124 Yusuke Imanaka[1], Maki Taniguchi[1], Takehiko Doi[1], Miyuki Tsumura[1], Rie Nagaoka[2], Maiko

125 Shimomura[1], Takaki Asano[1, 3Φ], Reiko Kagawa[1], Yoko Mizoguchi[1], Shuhei Karakawa[1], Koji Arihiro[4],

126 Kohsuke Imai[5], Tomohiro Morio[5], Jean-Laurent Casanova[3, 6, 7, 8], Anne Puel[3, 6, 7], Osamu Ohara[9],

127 Katsuhiko Kamei[10], Masao Kobayashi[1, 11Φ], Satoshi Okada[1]

128

129 **Institutions**

130 [1]Department of Pediatrics, Hiroshima University Graduate School of Biomedical and Health Science,

131 Hiroshima, Japan

132 [2]Division of Infectious Diseases Laboratory Medicine, Hiroshima University Hospital, Hiroshima, Japan

133 [3]St. Giles Laboratory of Human Genetics of Infectious Diseases, Rockefeller Branch, Rockefeller

134 University, New York, NY, United States

135 [4]Department of Anatomical Pathology, Hiroshima University Hospital, Hiroshima, Japan

136 [5]Department of Pediatrics and Developmental Biology, Graduate School of Medical and Dental Sciences,

137 Tokyo Medical and Dental University, Tokyo, Japan

[6]Laboratory of Human Genetics of Infectious Diseases, Necker Branch, INSERM UMR 1163, Imagine Institute, Paris, France

[7]University of Paris, Paris, France, EU

[8]Howard Hughes Medical Institute, New York, USA

[9]Department of Applied Genomics, Kazusa DNA Research Institute, Kisarazu, Japan

[10]Department of Medical Mycology Research Center, Chiba University, Japan

[11]Japan Red Cross, Chugoku-Shikoku Block Blood Center, Hiroshima, Japan

[Φ]current affiliation

Corresponding Author

Satoshi Okada, MD, PhD

Department of Pediatrics, Hiroshima University Graduate School of Biomedical and Health Sciences

1-2-3 Kasumi, Minami-Ku, Hiroshima-Shi, Hiroshima, 734-8551, Japan

Tell: +81-82-257-5212

Fax: +81-82-257-5214

E-mail: sokada@hiroshima-u.ac.jp

Abstract

Purpose

Autosomal recessive CARD9 deficiency predisposes patients to invasive fungal disease. *Candida* and *Trichophyton* species are major causes of fungal disease in these patients. Other CARD9-deficient patients display invasive disease caused by other fungi, such as *Exophiala spp*. The clinical penetrance of CARD9 deficiency regarding fungal disease is surprisingly not complete until adulthood, though the age remains unclear. Moreover, the immunological features of genetically confirmed yet asymptomatic individuals with CARD9 deficiency have not been reported.

Methods

Identification of *CARD9* mutations by gene panel sequencing and characterization of the cellular phenotype by quantitative PCR, immunoblot, luciferase reporter, and cytometric bead array assays were performed.

Results

Gene panel sequencing identified compound heterozygous *CARD9* variants, c.1118G>C (p.R373P) and c.586A>G (p.K196E), in a 4-year-old patient with multiple cerebral lesions and systemic lymphadenopathy due to *Exophiala dermatitidis*. The p.R373P is a known disease-causing variant, whereas the p.K196E is a private variant. Although the patient's siblings, a 10-year-old brother and an 8-year-old sister, were also compound heterozygous, they have been asymptomatic to date. Normal CARD9 mRNA and protein expression were found in the patient's $CD14^{+}$ monocytes. However, these cells exhibited markedly

impaired pro-inflammatory cytokine production in response to fungal stimulation. Monocytes from both asymptomatic siblings displayed the same cellular phenotype.

Conclusions

CARD9 deficiency should be considered in previously healthy patients with invasive *Exophiala dermatitidis* disease. Asymptomatic relatives of all ages should be tested for CARD9 deficiency. Detecting cellular defects in asymptomatic individuals is useful for diagnosing CARD9 deficiency.

Keywords: CARD9 deficiency, invasive fungal disease (IFD), *Exophiala dermatitidis*, asymptomatic siblings, cytokine production

Declarations

Funding

This study was supported by Grants-in-Aid for Scientific Research from the Japan Society for the Promotion of Science (16H05355 and 19H03620 to SO), Promotion of Joint International Research from the Japan Society for the Promotion of Science (18KK0228 to SO), and the Practical Research Project for Rare/Intractable Diseases from Japan Agency for Medical Research and Development, AMED (Grant Number: JP16ek0109179, JP19ek0109209, and JP20ek0109480) to S.O.

Conflicts of Interest

The authors declare that they have no conflicts of interest.

Availability of data and material

The datasets during and/or analyzed during the current study are available from the corresponding author on reasonable request.

Code availability

Not applicable

Authors' contributions

All authors contributed to the accrual of subjects and/or data. SO contributed to the conception and design of the study. YI, TA, AP, and JLC drafted the manuscript. YI, MT, RK, and YM performed cellular assay and gene expression experiment. MT, TD, RN, MS, SK, KA, KI, TM, KK, and MK performed the clinical work and collected data. OO and SO analyzed data obtained by gene panel sequencing. All authors have revised the manuscript for important intellectual content and approved the final version.

Ethics approval

210 The study was approved by the Ethics Committees and Institutional Review Board of Hiroshima University.

211 All experiments were carried out with adherence to the Declaration of Helsinki.

212

213 **Consent to participate**

214 Informed consent was obtained from the guardians of the pediatric patients or directly from participants.

215

216 **Consent for publication**

217 Informed consent was obtained from the guardians of the pediatric patients for publication of this case

218 report and accompanying images.

219

220 **Introduction**

221 Caspase-associated recruitment domain-9 (CARD9) deficiency is an autosomal recessive (AR) primary

222 immunodeficiency caused by loss-of-function mutations in the *CARD9* gene(1), which encodes a signaling

223 protein located downstream of C-type lectin receptors that recognizes fungal pathogen-associated

224 molecular patterns. Accordingly, AR CARD9 deficiency results in specific susceptibility to invasive and/or

225 superficial fungal disease (2, 3). Since its first report in 2009, AR CARD9 deficiency has been identified

226 in 78 patients from 55 kindreds from 17 countries, with 28 mutations identified as disease causing (1, 3-

227 20). With descriptions of an increasing number of patients, the clinical characteristics, pathophysiology,

228 and genetic background of AR CARD9 deficiency are gradually being deciphered. Nonetheless, many
229 questions remain unanswered (3).

230 AR CARD9 deficiency is characterized by invasive fungal diseases (IFD) that often affect the central
231 nervous system (CNS) (21). *Candida* and *Trychophyton* represent the two major disease-causing fungal
232 species in patients with AR CARD9 deficiency (Fig. S1) (3); *Aspergillus* (8, 14, 19, 22), *Auerobasidum*
233 (23), *Corynespora* (7, 24), *Exophiala* (13, 14, 17, 25), *Microsprorum* (9), *Mucor* (6), *Ochroconis* (17),
234 *Pallidocercospora* (11), *Phialophora* (10, 26), *Saprochaete* (15), and *Trichosporon* (4) species have less
235 frequently been reported. In particular, IFD caused by *Exophiala dermatitidis* has only been reported in 2
236 previously healthy patients with AR CARD9 deficiency at the ages of 8 and 23 years (13, 25).

237 Because all patients with disease-causing *CARD9* mutations develop fungal disease, the clinical
238 penetrance of AR CARD9 deficiency is thought to be complete (3). However, the age at onset ranges from
239 childhood to adulthood (3.5–58 years) (3, 27), suggesting that there are asymptomatic children or adults
240 who carry disease-causing mutations in *CARD9*, and such individuals are expected to develop fungal
241 disease later in life. Overall, the mortality rate of CARD9-deficient patients who develop IFD is >20% (3-
242 5, 7, 8, 12, 13, 15, 16, 18). Therefore, to reduce the mortality rate, it is important to diagnose patients with
243 AR CARD9 deficiency prior to the onset of IFD. Presymptomatic diagnosis of this disorder enables us to
244 monitor the patient closely and consider institutional therapy with antifungal prophylaxis. Although
245 diagnosing AR CARD9 deficiency is relatively easy when patients display characteristic clinical features

246 and carry previously reported disease-causing mutations, it becomes more challenging when patients
247 display an atypical clinical course, carry novel *CARD9* variants, or carry reported disease-causing mutations
248 but are asymptomatic.
249

250 **Materials and methods**

251 **Fungal identification**

252 PrepMan™ Ultra Sample Preparation Reagent (Applied Biosystems, Waltham, Massachusetts, USA) was
253 used to extract genomic DNA from a lymph node biopsy that was cultured in Sabouraud dextrose agar
254 according to the manufacturer's protocol. The DNA was amplified and sequenced from the D2 region of
255 the nuclear large subunit ribosomal RNA gene using MicroSEQ™ D2 rDNA Fungal Identification Kit
256 (Applied Biosystems) according to the manufacturer's protocol. For species assignment, sequences were
257 aligned using BLAST (NCBI, Washington, DC).
258

259 **DNA sequencing**

260 Genomic DNA was extracted from peripheral blood leukocytes and subjected to gene panel sequencing
261 and/or Sanger sequencing. The former revealed enriched PID-related genes reported in IUIS2017 (28). The
262 detailed method was described previously (29).
263

264 **Isolation of CD14$^+$ monocytes from peripheral whole blood**

265 Peripheral blood mononuclear cells (PBMCs) were isolated from peripheral whole blood by density
266 gradient centrifugation using Lymphoprep™ (Alere Technologies AS, Oslo, Norway). CD14$^+$ monocytes
267 were separated from PBMCs using IMag™ Cell Separation System (BD Biosciences, San Jose, CA, USA)
268 according to the manufacturer's protocol and resuspended in RPMI 1640 medium (Gibco, Thermo Fischer
269 Scientific, Waltham, MA, USA) supplemented with 10% heat-inactivated fetal bovine serum (FBS)
270 (HyClone, Logan, UT, USA) and 100 µg/ml penicillin/streptomycin.

271

272 **Quantitative PCR**

273 Total RNA was extracted from isolated CD14$^+$ monocytes with Qiagen RNeasy Mini kit (Qiagen, Hilden,
274 Germany) according to the manufacturer's protocol and transcribed by using Superscript III Reverse
275 Transcriptase (Invitrogen, Carlsbad, CA, USA). Quantitative PCR was performed in triplicate using
276 TaqMan primer/probe sets for *CARD9* (Hs00364485_m1), *GAPDH* (Hs99999905_m1) (Applied
277 Biosystems), TaqMan Fast Advanced Master Mix Reagents Kit (Applied Biosystems) according to the
278 manufacturer's protocol and the StepOne Real-Time PCR system (Applied Biosystems). GAPDH was used
279 as normalization control. The data were analyzed with the 2-ΔΔCT method.

280

281 **Immunoblot analysis**

282 Equal amounts of protein from isolated $CD14^+$ monocytes were separated by 10% SDS-PAGE and
283 transferred to PVDF membranes (Merck KgaA, Darmstadt, Germany). The membranes were blocked with
284 low-fat bovine milk. Proteins were probed with a rabbit anti-human CARD9 polyclonal antibody (Protein
285 Tech, Thermo Fisher Scientific, Waltham, MA, USA, catalog 10669-1-AP) or a mouse anti-ß-actin
286 monoclonal antibody (Sigma-Aldrich, St. Louis, MO, USA, catalog A5316). HRP-conjugated goat anti-
287 mouse and anti-rabbit antibodies (GE Healthcare, Buckinghamshire, England, UK) were used as secondary
288 antibodies. Antibody binding was detected using enhanced chemiluminescence reagent (Thermo Fisher
289 Scientific, Waltham, MA, USA), and the band intensity was quantified using ImageJ software (National
290 Institutes of Health, Bethesda, MD).
291
292 **Mutagenesis and transient transfections**
293 We used pcDNA3.1 V5-His-wild-type (WT)-*CARD9* and -mutant-*CARD9* (p.R35Q and p.R70W), as
294 described previously (21), for this study. We generated expression vectors encoding p.K196E and p.R373P
295 CARD9 variants using PCR-based mutagenesis of the pcDNA3.1 V5-His-WT-*CARD9* vector with
296 mismatched PCR primers. The primer sequences and PCR conditions are available upon request.
297 HEK293T cells were plated for 18 h in 6-well plates at 7.5×10^5 cells/well in DMEM (Gibco) supplemented
298 with 100 µg/ml penicillin/streptomycin. Then, plasmids carrying the WT *CARD9* allele or each mutant
299 *CARD9* allele were used to transfect HEK293T cells with Lipofectamine LTX Reagent (Thermo Fisher

300 Scientific) according to the manufacturer's protocol. After 24 h, the transfected HEK293T cells were

301 subjected to immunoblot analysis.

302

303 **Luciferase reporter assay**

304 HEK293T cells were plated for 18 h in 96-well plates at 2.5×10^4 cells/well in DMEM (Gibco) supplemented

305 with 100 μg/ml penicillin/streptomycin. The cells were transfected with *DECTIN*-, *SYK*-, and *BCL*10-

306 expressing pcDNA3.1 vectors with the WT *CARD9*- or mutant *CARD9* (p.R70W, p.K196E or p.R373P)-

307 expressing pcDNA3.1 vector, Igkcona-Luc (provided by S. Yamaoka) and pRL-TK (Promega, Madison,

308 Wisconsin, USA) using Lipofectamine LTX Reagent according to the manufacturer's protocol. The cells

309 were stimulated with heat-killed *Exophiala dermatitidis* (1×10^6 particles/well) for 24 h. Luciferase reporter

310 gene activities were determined with Dual-Luciferase Reporter Assay System (Promega). The experiments

311 were performed in triplicate, and data are expressed in relative luciferase units (RLU).

312

313 **Cytokine analysis**

314 Isolated $CD14^+$ monocytes were cultured in 96-well plates at 4×10^4 cells/well in RPMI 1640 medium and

315 stimulated with lipopolysaccharide (LPS) (from *Escherichia coli*, serotype O111: B4; Sigma-Aldrich) (10

316 ng/ml) for 2 h or with heat-killed *Candida albicans* (1×10^6 particles/well), heat-killed *Candida glabrata*

317 (1×10^6 particles/well), or heat-killed *Exophiala dermatitidis* (1×10^6 particles/well) for 24 h. The details of

318 heat-killed fungus preparation are described previously (30). Cytokine levels (TNF-α, IL-6) were measured
319 in the culture supernatants using a cytometric bead array (CBA) (BD Biosciences) and analyzed according
320 to the manufacturer's instructions using CBA Flex Set (BD Biosciences). The experiments were performed
321 in triplicate.
322
323 **Results**
324 **Case report**
325 The patient was a previously healthy 4-year-old Japanese girl born to non-consanguineous parents. There
326 was no history of any severe disease in her parents or her two siblings, a 10-year-old brother and an 8-year-
327 old sister. She received all the vaccines for her age, according to the recommendation by the Japan Pediatric
328 Society, without any adverse effects.
329 At the age of 4 years, she was hospitalized with speech disorder and right hemiparesis that continued for
330 one month. Physical examination showed muscle weakness in the right upper and lower limbs.
331 Lymphadenopathies in the supraclavicular and axillary regions (10 mm) and a mass in the abdomen (30
332 mm) were also noted. Brain magnetic resonance imaging (MRI) revealed multiple masses up to 20 mm in
333 diameter on the left side of the cerebellum, mesencephalon, temporal lobe and basal ganglia (Fig. 1Aa, b).
334 Chest and abdominal computed tomography (CT) scans showed supraclavicular, axillary, and intra-
335 abdominal lymphadenopathies and multiple low-density lesions in the spleen (Fig. 1Ac, d). Cerebrospinal

336 fluid (CSF) leukocyte counts were normal, as were CSF levels of protein and glucose. Blood and CSF
337 cultures were negative for bacterial, fungal, and acid-fast bacilli; gastric juice culture was also negative for
338 acid-fast bacilli. Interferon-gamma release assays (IGRAs) showed negative results, ruling out
339 *Mycobacterium tuberculosis* infection. Based on histopathology of the axillary lymph nodes, necrotizing
340 granuloma with low neutrophil infiltration was present (Fig. 1Ba, b). Periodic acid Schiff (PAS) and
341 Grocott staining revealed yeast-like fungi (Fig. 1Bc, d). *Exophiala dermatitidis* was suspected by direct
342 microscopic examination of the fungal culture (Fig. 1C) and was confirmed by sequencing the D2 region
343 of the large subunit ribosomal RNA gene. The patient was thus diagnosed with invasive
344 phaeohyphomycosis (brain, lymph nodes, spleen) due to *E. dermatitidis*.
345 The patient was initially treated with a 16-mg voriconazole/kg/day infusion as empiric therapy. Her
346 symptoms gradually improved with a month of treatment, though with little impact on the multiple cerebral
347 lesions and systemic lymphadenopathies. She then received 2.5 mg liposomal amphotericin B/kg/day in
348 addition to voriconazole based on the identification and drug sensitivity of *E. dermatitidis*, and the multiple
349 cerebral lesions and systemic lymphadenopathy gradually improved. After 5 months of administration of
350 liposomal amphotericin B, the multiple cerebral lesions shrank and stabilized, but not fully disappeared.
351 Then the patient was subsequently treated with oral 800 mg voriconazole, and 125 mg terbinafine has been
352 continued to date. Follow-up at 2 years indicated no evidence of recurrence.
353

354 **Identification of *CARD9* variants**

355 Due to the IFD caused by *E. dermatitidis* in this otherwise healthy 4-year-old girl, we suspected the
356 possibility of an inborn error of immunity and performed gene panel sequencing. After the filtering process
357 (minor allele frequency (MAF) <0.01), 15 rare variants were identified (Table S1). Among them, rare
358 variants in *AK2*, *BCL11B, IL10RA, IL17RC, IRAK1, KMT2D, LRBA, ORAI1, PRF1, SH3BP2,* and
359 *SLC29A3* were unlikely to be disease causing based on their inheritance patterns or the patient's clinical
360 phenotype. As no other candidate rare variants that could explain the patient's manifestations were
361 identified by gene panel sequencing, two variants, c.586A>G (p.K196E) and c.1118G>C (p.R373P), of
362 *CARD9* (Fig. 2) were considered to be the best candidates. Both variants were confirmed by Sanger
363 sequencing (Fig. 3A). The p.K196E variant, which was inherited from her asymptomatic mother, has never
364 been reported. In contrast, the p.R373P variant, inherited from her asymptomatic father, has previously
365 been reported as disease causing, either in the homozygous or compound heterozygous state (9, 11, 31).
366 The patient's 10-year-old brother and 8-year-old sister were totally asymptomatic, even though they were
367 both compound heterozygous for CARD9 p.K196E and p.R373P, similarly to their affected sister (Fig. 3B).
368 Computational assessment of the predicted pathological significance of these two variants using combined
369 annotation-dependent depletion (CADD) showed that their CADD scores (p.K196E: 22.9; p.R373P: 16.0)
370 were higher than the 99% confidence mutation significant cutoff (MSC: 10.26) (32-34); in addition, a low
371 MAF (p.K196E: 4.4×10^{-5}; p.R373P: 2.3×10^{-5}) in the general population was determined for both. These

372 compound heterozygous variants were thus expected to be very rare, even though each MAF was not much
373 different from that of heterozygous variants reported in the general population (Fig. S2). Moreover, disease-
374 causing nonsense, frameshift, and essential splicing mutations showed lower MAFs and/or higher CADD
375 scores than the homozygous variants reported in the general population. In contrast, some disease-causing
376 missense variants, including the two identified variants p.K196E and p.R373P, had MAFs and/or CADD
377 scores equivalent to those of some homozygous variants reported in the general population (Fig. 3C).
378 Collectively, these data suggest that the identified biallelic *CARD9* variants are disease causing and
379 strengthen the importance of functional testing to validate the pathogenicity of identified variants.
380
381 ***CARD9* mRNA and protein expression**
382 We first investigated *CARD9* mRNA expression levels in peripheral blood by quantitative PCR. *CARD9*
383 mRNA was strongly expressed in the neutrophils, monocytes, and natural killer (NK) cells of healthy
384 donors (Fig. S3). Therefore, we assessed *CARD9* mRNA levels in the $CD14^+$ monocytes of the patient and
385 found levels comparable to those of two controls tested in parallel (Fig. 4A). We next assessed CARD9
386 protein expression in her $CD14^+$ monocytes by immunoblotting and found levels similar to those of control
387 cells (Fig 4B, C). Taken together, the biallelic variants of *CARD9* did not affect mRNA or protein
388 expression in the patient's cells. To confirm these findings, we transiently expressed WT or mutant
389 p.K196E, p.R373P, p.R35Q, or p.R70W *CARD9* alleles in HEK293T cells; p.R35Q and p.R70W have

390 previously been reported as disease causing (8, 18, 21, 35). In cells transfected with the p.K196E or
391 p.R373P allele, CARD9 protein levels were similar to those in cells transfected with the WT, p.R35Q, or
392 p.R70W allele (Fig. 4D, E).
393
394 **Functional impact of p.K196E and p.R373P *CARD9* alleles**
395 We next evaluated the functional impact of each *CARD9* allele using an NF-κB reporter assay, as previously
396 reported (21). In cells transfected with the *CARD9* p.K196E or p.R373P allele, NF-κB transcriptional
397 activity was comparable to that in cells transfected with the WT allele, both at the basal level and after
398 stimulation with *E. dermatitidis*. In contrast, cells transfected with the *CARD9* p.R70W allele displayed
399 impaired NF-κB transcriptional activity, consistent with a previous report (Fig. 4F) (21). Therefore, the
400 NF-κB reporter assay using HEK293T cells did not allow us to draw a conclusion about the impact of the
401 identified CARD9 variants, and further analyses were carried out.
402
403 **Cytokine production in response to fungal stimulation**
404 We next evaluated the biological impact of the p.K196E and p.R373P variants by measuring the production
405 of pro-inflammatory cytokines from $CD14^+$ monocytes from the patient, patient's mother's or siblings
406 stimulated with heat-killed *C. albicans*, *C. glabrata*, *E. dermatitidis* and LPS. The patient's $CD14^+$
407 monocytes (p.K196E/p.R373P) displayed markedly impaired TNF-α and IL-6 production after stimulation

408 with *C. albicans*, *C. glabrata*, and *E. dermatitidis* compared with cells from healthy controls (Fig. 5A, B).

409 In contrast, cytokine production following LPS stimulation was normal in the patient's $CD14^+$ monocytes.

410 Similarly, the $CD14^+$ monocytes from the patient's asymptomatic siblings (p.K196E/p.R373P) were also

411 markedly impaired in TNF-α and IL-6 production in response to fungal stimulation, which were normal in

412 response to LPS. The $CD14^+$ monocytes from the patient's mother (p.K196E/WT) displayed an

413 intermediate cellular phenotype; cells from her father (p.R373P/WT) were not available. Altogether, these

414 results showed monocytes carrying biallelic variants, p.K196E/p.R373P, to be impaired with regard to

415 TNF-α and IL-6 production in response to various fungal ligands but normal in response to LPS. These *ex*

416 *vivo* observations, together with the clinical manifestations of the patient, suggested that both *CARD9*

417 mutations are pathogenic.

418

419 **Immunological findings**

420 The immunological findings for the patient at the age of 4 (before starting antifungal treatment) and 5 (after

421 treatment) years are shown in Tables S1 and S2. Briefly, blood analysis indicated normal percentages of

422 neutrophils, monocytes, and lymphocytes; however, leukocyte counts were high at 15,540/mm^3, and the

423 percentages of eosinophils were also high, at 26.1%, before treatment. The serum level of IgE was normal,

424 whereas that of IgG was high at 4,254 mg/dL. The leukocytosis, including eosinophilia, and elevated IgG

425 resolved after antifungal treatments. T lymphocyte proliferation was normal in response to PHA and Con-

426 A. In addition, the leukocyte oxidative burst, as assessed by the dihydrorhodamine (DHR) test, was normal.

427 HIV infection was ruled out by laboratory testing. Furthermore a detailed lymphocyte subpopulation

428 analysis was performed by multicolor flow cytometry, as previously described (36), and the percentages of

429 T, B, and NK cells were within the normal ranges; however, slightly decreased Th17 cell ($CCR6^{+}CXCR3^{-}$

430 $/CD3^{+}CD4^{+}CD45RO^{+}$) percentages were noticed.

431 Immunological findings for the patient's brother (at 12 years) and sister (at 11 years) as well as her mother

432 are shown in Tables S1 and S2. Briefly, blood analysis in the patient's siblings revealed normal percentages

433 of leukocytes, neutrophils, lymphocytes, and monocytes, though the percentages of eosinophils in her

434 brother were slightly high at 8.9%; serum levels of IgE in the brother and sister were also high, at 339

435 IU/mL and 342 IU/mL, respectively. The percentages of T cells, B cells, and NK cells in the patient's

436 siblings and mother were within normal ranges, with no decrease in Th17 cell counts.

437

438 **Discussion**

439 We report a patient with compound heterozygous *CARD9* mutations who developed IFD caused by *E.*

440 *dermatitidis*, a dematiaceous fungus distributed in the environment (37). Although *E. dermatitidis* is found

441 worldwide, it is particularly common in East Asia (38). *E. dermatitidis* is a pathogen that causes a number

442 of clinical manifestations of phaeohyphomycosis, including skin, subcutaneous, and sinus infections. In

443 rare instances, it can cause invasive phaeohyphomycosis in the CNS and liver (13). In a summary report of

444 43 patients with invasive phaeohyphomycosis caused by *E. dermatitidis*, the state of secondary
445 immunosuppression, including presenting with malignant tumors, cystic fibrosis, and steroid treatment,
446 was reported to involve host factors in 18 patients. Moreover, primary immunodeficiency (AR CARD9
447 deficiency in 1 patient and chronic granulomatous disease in 1 patient (39)) was reported as a host factor;
448 no known host factors were reported for the other 23 cases (25). In patients with primary immunodeficiency,
449 the onset of invasive phaeohyphomycosis caused by *E. dermatitidi*s has only been reported in 1 additional
450 patient aside from those previously mentioned, and this patient was diagnosed with AR CARD9 deficiency
451 (13). Among two patients with AR CARD9 deficiency, one died by severe pneumonia and central nervous
452 infection which resulted in brain herniation (13). The other patient developed IFD, but successfully treated
453 with antifungal therapy. She is alive, although she experienced the recurrence of invasive
454 phaeohyphomycosis caused by *E. dermatitidis* in spite of antifungal prophylaxis (25). Therefore, our case
455 is the third report of invasive phaeohyphomycosis caused by *E. dermatitidis* in association with AR CARD9
456 deficiency. The target organs in our patient were the brain, systemic lymph nodes, and spleen. The
457 histopathology of the lymph nodes in our patient showed not only the presence of fungi, but also necrotizing
458 granuloma with low neutrophil infiltration. These findings are consistent to the previous studies which
459 described impaired neutrophil infiltration to the infection sites, such as CSF (21, 31, 40), skin (17, 19, 37),
460 lymph node (22), and adrenal masses (22), in patients with AR CARD9 deficiency. Lack of CXC-
461 chemokine induction at the infection sites have been reported as a cause of impaired neutrophil infiltration

462 (40, 41). CNS disease was reported in both patients with AR CARD9 deficiency who developed invasive

463 *E. dermatitidis* disease (13, 25). Nevertheless, fungal disease of the CNS has been frequently reported in

464 patients with AR CARD9 deficiency; among 26 patients who developed invasive *Candida* species disease,

465 20 (76.9%) developed CNS disease (3, 4, 8, 16, 18, 23). Overall, it is suspected that many patients who

466 develop invasive phaeohyphomycosis caused by *E. dermatitidi*s without known host factors have not

467 undergone genetic evaluations. Among these, AR CARD9 deficiency may require differentiation,

468 particularly in patients with CNS disease.

469 In our patient, AR CARD9 deficiency was diagnosed based on the presence of various symptoms,

470 identification of *CARD9* mutations and impaired production of pro-inflammatory cytokines specific to

471 fungal stimulation in $CD14^+$ monocytes. Although p.K196E and p.R373P, identified in our patient, are

472 considered loss-of-function mutations, impaired function caused by each mutation could not be adequately

473 evaluated *in vitro* or computational analysis, MAFs and CADD scores. The *CARD9* gene contains 13 exons;

474 the encoded protein has CARD and coiled-coil (CC) domains (42). The mutation p.K196E located in exon

475 4 within the CC domain and p.R373P in exon 8 within the CC domain. p.K196E is a novel mutation,

476 whereas p.R373P is a known disease-causing mutation identified in 3 patients from 3 kindreds (9, 11, 31).

477 CARD9 protein expression in patients with p.R373P homozygous mutations is reportedly normal (11),

478 though it is impaired in patients with p.R373P/p.G72S compound heterozygous mutations (31).

479 Accordingly, there is no consensus on the effect of p.R373P mutation on CARD9 protein expression. In

480 our patient, levels of both CARD9 mRNA and protein expression were normal; hence, p.R373P was
481 determined to be normally expressed at the protein level. The transient gene expression experiment
482 confirmed this finding. Indeed, both p.K196E and p.R373P alleles were normally expression in protein
483 level. Subsequently, we sought to assess the pathological significance of p.K196E and p.R373P mutations
484 using transient gene expression experiments; however, the results of NF-κB transcriptional activity
485 assessment failed to demonstrate dysfunction. Previous study investigated *CARD9* mutants in CARD
486 domain (p.R18W, p.R35Q, and p.R70W) and CC domain (p.Q289* and p.Q295*) by NF-κB transcriptional
487 activity. This assay revealed impaired NF-κB activity in three mutations in CARD domain, whereas two
488 mutations in CC domain predicted to have normal activity (21, 25). Since two mutations in CC domain are
489 nonsense and recurrently found in patients with IFD, they should be pathogenic. Therefore, NF-kB reporter
490 assay might not be suitable for evaluating pathogenicity of mutations in CC domain. We thus suspect that
491 NF-kB reporter assay failed to confirm the pathogenicity of p.R373P and p.K196E allele because they
492 locate in CC domain. Including our study, there have been no *in vitro* evaluations that can accurately
493 measure the effects of *CARD9* mutations, and this is a topic for future study.
494 Although our patient's siblings, a 10-year-old brother and an 8-year-old sister, did not develop fungal
495 disease, similar to the patient, both harbored p.K196E/p.R373P *CARD9* mutations. Thus, asymptomatic
496 siblings of all ages should be tested for AR CARD9 deficiency. Because cases of adulthood onset have
497 been reported, it is possible that there are individuals with AR CARD9 deficiency who do not develop

498 fungal disease in childhood. Nonetheless, there have been no reports to date on detailed investigations in
499 presymptomatic individuals carrying disease-causing *CARD9* mutations. Indeed, this is the first report of
500 impaired production of pro-inflammatory cytokines against fungi in a patient prior to the onset of fungal
501 disease. This may fit with a previous observation which described complete penetrance of AR CARD9
502 deficiency (3). We started antifungal prophylaxis with oral fluconazole (100 mg/day) and close monitoring
503 of patient's siblings because they are considered at high risk for future fungal disease. After starting
504 prophylaxis, they have no episodes of fungal infections. On the other side, we need to say that there still
505 remains a possibility that the penetrance of AR CARD9 deficiency is not complete because some of the
506 patients with AR CARD9 deficiency are asymptomatic until middle age (3). Further accumulation of the
507 cases is required to fully understand a global epidemiology of this disorder. Regardless of the presence or
508 absence of fungal disease, a reduction in the production of pro-inflammatory cytokines was demonstrated
509 in this study by using a cellular assay for $CD14^{+}$ monocytes from both patients and presymptomatic
510 individuals, and this evaluation system might be used to assess the biological effects of *CARD9* variants of
511 unknown pathological significance identified using comprehensive genetic analyses.
512
513 **Appendix**
514
515 **Acknowledgment**

The sequence analysis was supported by the Analysis Center of Life Science, Natural Science Center for Basic Research and Development, Hiroshima University.

References

1. Glocker EO, Hennigs A, Nabavi M, Schaffer AA, Woellner C, Salzer U, et al. A homozygous CARD9 mutation in a family with susceptibility to fungal infections. N Engl J Med. 2009;361(18):1727-35.

2. Shiokawa M, Yamasaki S, Saijo S. C-type lectin receptors in anti-fungal immunity. Curr Opin Microbiol. 2017;40:123-30.

3. Corvilain E, Casanova JL, Puel A. Inherited CARD9 Deficiency: Invasive Disease Caused by Ascomycete Fungi in Previously Healthy Children and Adults. J Clin Immunol. 2018;38(6):656-93.

4. Quan C, Li X, Shi RF, Zhao XQ, Xu H, Wang B, et al. Recurrent fungal infections in a Chinese patient with CARD9 deficiency and a review of 48 cases. Br J Dermatol. 2019;180(5):1221-5.

5. Sari S, Dalgic B, Muehlenbachs A, DeLeon-Carnes M, Goldsmith CS, Ekinci O, et al. Prototheca zopfii Colitis in Inherited CARD9 Deficiency. J Infect Dis. 2018;218(3):485-9.

6. Wang X, Wang A, Wang X, Li R, Yu J. Cutaneous mucormycosis caused by Mucor irregularis in a patient with CARD9 deficiency. Br J Dermatol. 2019;180(1):213-4.

7. Arango-Franco CA, Moncada-Velez M, Beltran CP, Berrio I, Mogollon C, Restrepo A, et al. Early-Onset Invasive Infection Due to Corynespora cassiicola Associated with Compound Heterozygous CARD9 Mutations in a Colombian Patient. J Clin Immunol. 2018;38(7):794-803.

8. De Bruyne M, Hoste L, Bogaert DJ, Van den Bossche L, Tavernier SJ, Parthoens E, et al. A CARD9 Founder Mutation Disrupts NF-kappaB Signaling by Inhibiting BCL10 and MALT1 Recruitment and Signalosome Formation. Front Immunol. 2018;9:2366.

9. Zhang Y, Mijiti J, Huang C, Song Y, Wan Z, Li R, et al. Deep dermatophytosis caused by Microsporum ferrugineum in a patient with CARD9 mutations. Br J Dermatol. 2019;181(5):1093-5.

10. Huang C, Zhang Y, Song Y, Wan Z, Wang X, Li R. Phaeohyphomycosis caused by Phialophora americana with CARD9 mutation and 20-year literature review in China. Mycoses. 2019;62(10):908-19.

11. Guo Y, Zhu Z, Gao J, Zhang C, Zhang X, Dang E, et al. The Phytopathogenic Fungus Pallidocercospora crystallina-Caused Localized Subcutaneous Phaeohyphomycosis in a Patient with a Homozygous Missense CARD9 Mutation. J Clin Immunol. 2019;39(7):713-25.

546 12. Nazarian RM, Lilly E, Gavino C, Hamilos DL, Felsenstein D, Vinh DC, et al. Novel CARD9
547 mutation in a patient with chronic invasive dermatophyte infection (tinea profunda). J Cutan Pathol.
548 2020;47(2):166-70.
549 13. Wang C, Xing H, Jiang X, Zeng J, Liu Z, Chen J, et al. Cerebral Phaeohyphomycosis Caused by
550 Exophiala dermatitidis in a Chinese CARD9-Deficient Patient: A Case Report and Literature Review. Front
551 Neurol. 2019;10:938.
552 14. Perez L, Messina F, Negroni R, Arechavala A, Bustamante J, Oleastro M, et al. Inherited CARD9
553 Deficiency in a Patient with Both Exophiala spinifera and Aspergillus nomius Severe Infections. J Clin
554 Immunol. 2020;40(2):359-66.
555 15. Erman B, Firtina S, Aksoy BA, Aydogdu S, Genc GE, Dogan O, et al. Invasive Saprochaete
556 capitata Infection in a Patient with Autosomal Recessive CARD9 Deficiency and a Review of the Literature.
557 J Clin Immunol. 2020;40(3):466-74.
558 16. Du B, Shen N, Hu J, Tao Y, Mo X, Cao Q. Complete clinical remission of invasive Candida
559 infection with CARD9 deficiency after G-CSF treatment. Comp Immunol Microbiol Infect Dis.
560 2020;70:101417.
561 17. Wang X, Zhang R, Wu W, Song Y, Wan Z, Han W, et al. Impaired Specific Antifungal Immunity
562 in CARD9-Deficient Patients with Phaeohyphomycosis. J Invest Dermatol. 2018;138(3):607-17.
563 18. Martin S, Balligand E, Peeters J, Nassogne MC, Mondovits B, Loop M, et al. A 7-Year-Old
564 Child With Headaches and Prolonged Fever Associated With Oral and Nail Lesions. Open Forum Infect
565 Dis. 2019;6(11):ofz229.
566 19. Zhang Y, Huang C, Song Y, Ma Y, Wan Z, Zhu X, et al. Primary Cutaneous Aspergillosis in a
567 Patient with CARD9 Deficiency and Aspergillus Susceptibility of Card9 Knockout Mice. J Clin Immunol.
568 2020.
569 20. Queiroz-Telles F, Mercier T, Maertens J, Sola CBS, Bonfim C, Lortholary O, et al. Successful
570 Allogenic Stem Cell Transplantation in Patients with Inherited CARD9 Deficiency. J Clin Immunol.
571 2019;39(5):462-9.
572 21. Lanternier F, Mahdaviani SA, Barbati E, Chaussade H, Koumar Y, Levy R, et al. Inherited
573 CARD9 deficiency in otherwise healthy children and adults with Candida species-induced
574 meningoencephalitis, colitis, or both. J Allergy Clin Immunol. 2015;135(6):1558-68 e2.
575 22. Rieber N, Gazendam RP, Freeman AF, Hsu AP, Collar AL, Sugui JA, et al. Extrapulmonary
576 Aspergillus infection in patients with CARD9 deficiency. JCI Insight. 2016;1(17):e89890.
577 23. Gavino C, Mellinghoff S, Cornely OA, Landekic M, Le C, Langelier M, et al. Novel bi-allelic
578 splice mutations in CARD9 causing adult-onset Candida endophthalmitis. Mycoses. 2017;12:3218-21.
579 24. Yan XX, Yu CP, Fu XA, Bao FF, Du DH, Wang C, et al. CARD9 mutation linked to Corynespora
580 cassiicola infection in a Chinese patient. Br J Dermatol. 2016;174(1):176-9.

581 25. Lanternier F, Barbati E, Meinzer U, Liu L, Pedergnana V, Migaud M, et al. Inherited CARD9
582 deficiency in 2 unrelated patients with invasive Exophiala infection. J Infect Dis. 2015;211(8):1241-50.
583 26. Wang X, Wang W, Lin Z, Wang X, Li T, Yu J, et al. CARD9 mutations linked to subcutaneous
584 phaeohyphomycosis and TH17 cell deficiencies. J Allergy Clin Immunol. 2014;133(3):905-8 e3.
585 27. Puel A. Human inborn errors of immunity underlying superficial or invasive candidiasis. Hum
586 Genet. 2020;139(6):1011-22.
587 28. Bousfiha A, Jeddane L, Picard C, Ailal F, Bobby Gaspar H, Al-Herz W, et al. The 2017 IUIS
588 Phenotypic Classification for Primary Immunodeficiencies. J Clin Immunol. 2018;38(1):129-43.
589 29. Fujiki R, Ikeda M, Yoshida A, Akiko M, Yao Y, Nishimura M, et al. Assessing the Accuracy of
590 Variant Detection in Cost-Effective Gene Panel Testing by Next-Generation Sequencing. J Mol Diagn.
591 2018;20(5):572-82.
592 30. Liang P, Wang X, Wang R, Wan Z, Han W, Li R. CARD9 deficiencies linked to impaired
593 neutrophil functions against Phialophora verrucosa. Mycopathologia. 2015;179(5-6):347-57.
594 31. Drewniak A, Gazendam RP, Tool AT, van Houdt M, Jansen MH, van Hamme JL, et al. Invasive
595 fungal infection and impaired neutrophil killing in human CARD9 deficiency. Blood. 2013;121(13):2385-
596 92.
597 32. Itan Y, Shang L, Boisson B, Ciancanelli MJ, Markle JG, Martinez-Barricarte R, et al. The
598 mutation significance cutoff: gene-level thresholds for variant predictions. Nat Methods. 2016;13(2):109-
599 10.
600 33. Zhang P, Bigio B, Rapaport F, Zhang SY, Casanova JL, Abel L, et al. PopViz: a webserver for
601 visualizing minor allele frequencies and damage prediction scores of human genetic variations.
602 Bioinformatics. 2018;34(24):4307-9.
603 34. Rentzsch P, Witten D, Cooper GM, Shendure J, Kircher M. CADD: predicting the
604 deleteriousness of variants throughout the human genome. Nucleic Acids Res. 2019;47(D1):D886-D94.
605 35. Alves de Medeiros AK, Lodewick E, Bogaert DJ, Haerynck F, Van Daele S, Lambrecht B, et al.
606 Chronic and Invasive Fungal Infections in a Family with CARD9 Deficiency. J Clin Immunol.
607 2016;36(3):204-9.
608 36. Takashima T, Okamura M, Yeh TW, Okano T, Yamashita M, Tanaka K, et al. Multicolor Flow
609 Cytometry for the Diagnosis of Primary Immunodeficiency Diseases. J Clin Immunol. 2017;37(5):486-95.
610 37. Kirchhoff L, Olsowski M, Rath PM, Steinmann J. Exophiala dermatitidis: Key issues of an
611 opportunistic fungal pathogen. Virulence. 2019;10(1):984-98.
612 38. Sudhadham M, Prakitsin S, Sivichai S, Chaiyarat R, Dorrestein GM, Menken SB, et al. The
613 neurotropic black yeast Exophiala dermatitidis has a possible origin in the tropical rain forest. Stud Mycol.
614 2008;61:145-55.

615 39. Kenny RT, Kwon-Chung KJ, Waytes AT, Melnick DA, Pass HI, Merino MJ, et al. Successful
616 treatment of systemic Exophiala dermatitidis infection in a patient with chronic granulomatous disease.
617 Clin Infect Dis. 1992;14:235-42
618 .
619 40. Drummond RA, Collar AL, Swamydas M, Rodriguez CA, Lim JK, Mendez LM, et al. CARD9-
620 Dependent Neutrophil Recruitment Protects against Fungal Invasion of the Central Nervous System. PLoS
621 Pathog. 2015;11(12):e1005293.
622 41. Drummond RA, Swamydas M, Oikonomou V, Zhai B, Dambuza IM, Schaefer BC, et al.
623 CARD9(+) microglia promote antifungal immunity via IL-1beta- and CXCL1-mediated neutrophil
624 recruitment. Nat Immunol. 2019;20(5):559-70.
625 42. Bertin J, Guo Y, Wang L, Srinivasula SM, Jacobson MD, Poyet JL, et al. CARD9 is a novel
626 caspase recruitment domain-containing protein that interacts with BCL10/CLAP and activates NF-kappa
627 B. J Biol Chem. 2000;275(52):41082-6.

628

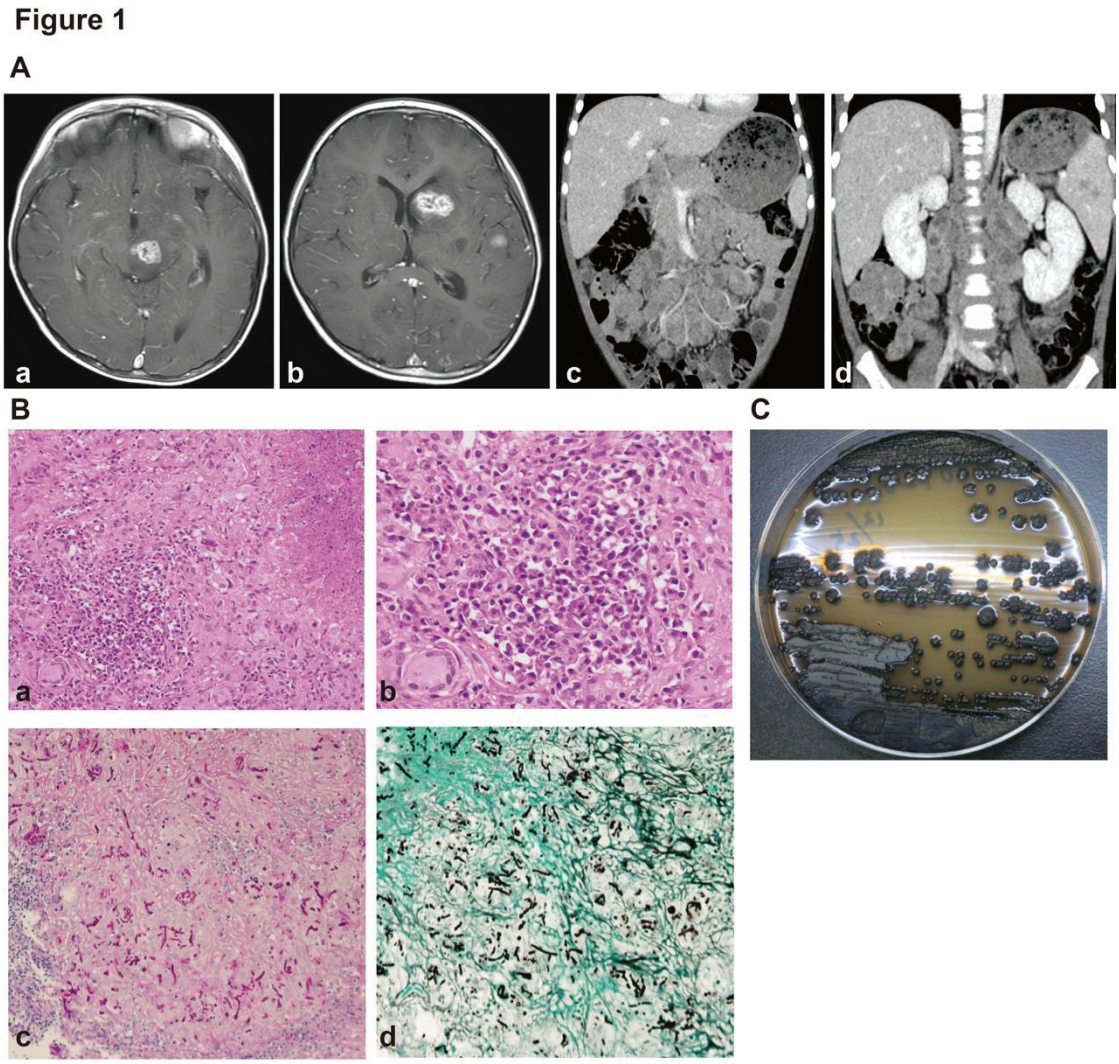

Figure 1

Image findings and features of the fungus infecting the patient. **A** Radiological examination of the patient. **a** and **b** Brain MRI showed high-intensity lesions on the left side of the mesencephalon, temporal lobe and basal ganglia. **c** and **d** Abdominal CT scan showed multiple intra-abdominal lymphadenopathies and multiple low-density lesions in the spleen. **B** Histopathological and microbiological features of the fungus in the patient. **a** and **b** Hematoxylin-eosin staining of the lymph node biopsy specimen showed necrotizing granulomas with low neutrophil infiltration (**a** 200×, **b** 400×). **c** and **d** Fungi were noted in the lymph node

biopsy by Periodic acid Schiff and Grocott staining, respectively (**c** 200×, **d** 400×). **C** Macroscopic appearance of the fungus. Rough colonies of black color on Sabouraud dextrose agar.

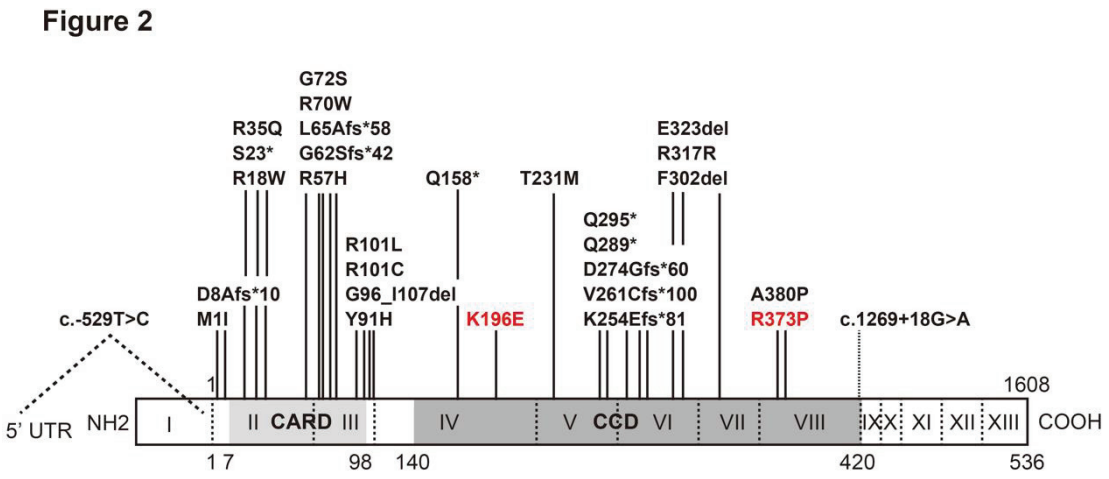

641

642 **Figure 2**

643 Schematic representation of the human CARD9 protein with the CARD domain (residues 7-98) and coiled-

644 coiled domain (CCD) (residues 140-420). The proband's variants (p.K196E and p.R373P) are shown in red,

645 among other previously reported pathogenic mutations. The 13 exons are indicated by Roman numerals,

646 and the first exon is nonprotein coding.

647

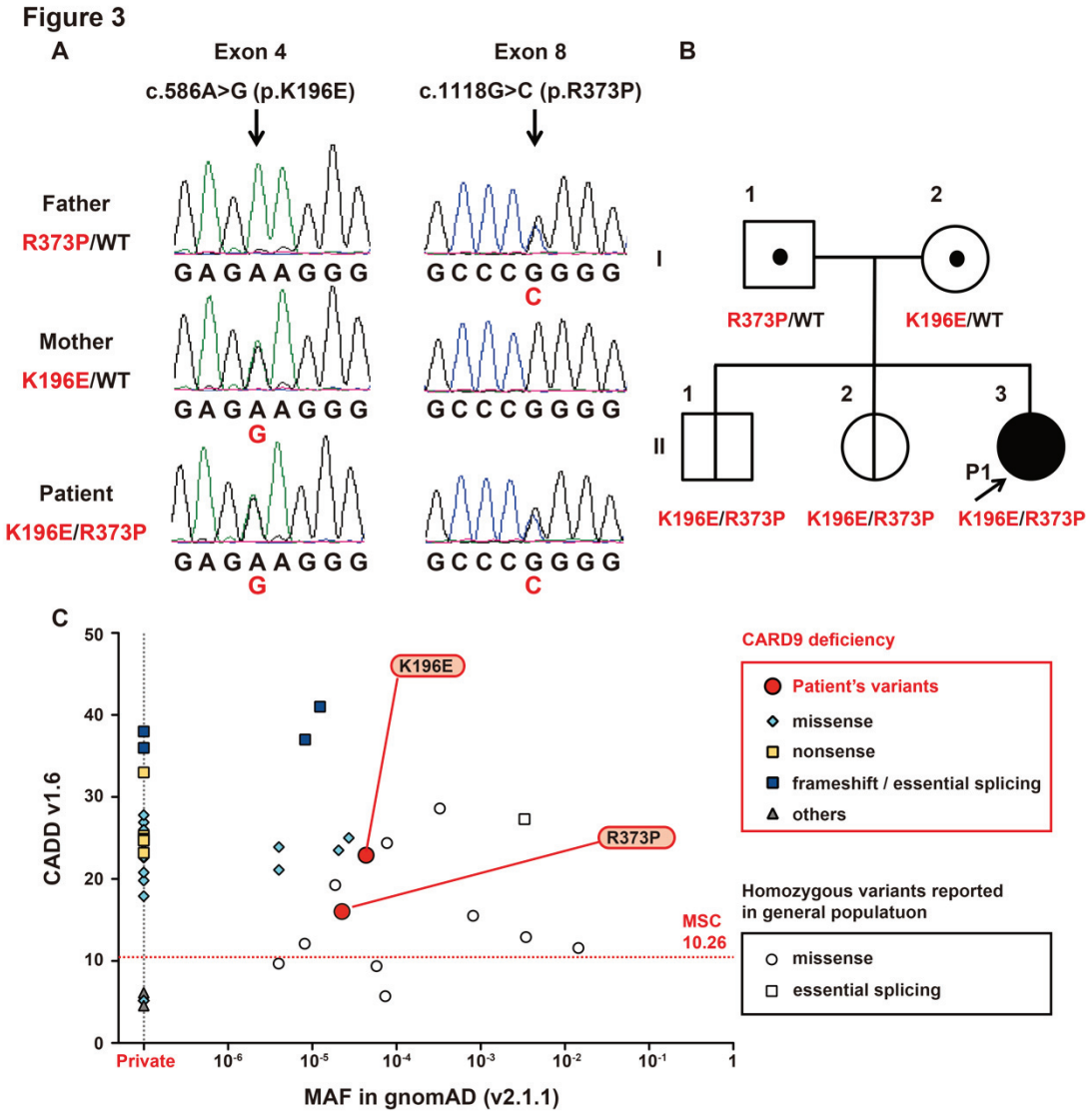

Figure 3

Identification of *CARD9* variants and computational analysis. **A** Sanger sequencing results. The heterozygous p.K196E variant in exon 4 was present in the patient and her mother. The heterozygous p.R373P variant in exon 8 was present in the patient and her father. **B** Pedigree of the family. The arrow indicates the proband. **C** *In silico* analysis of *CARD9* variants. The graph shows the MAF and CADD v1.6 scores for disease-causing mutations previously reported in AR CARD9 deficiency and homozygous

655 variants in the general population, gnomAD v2.1.1 (https://gnomad.broadinstitute.org). The red dotted line

656 shows the CADD-MSC score (99% confidence interval) for *CARD9*. The variants identified in our patient

657 are indicated in red circles. Missense, nonsense, frameshift/essential splicing, and UTR (others) mutations

658 reported in AR CARD9 deficiency are indicated by light blue diamonds, yellow squares, blue squares, and

659 black triangles, respectively. Homozygous missense and essential splicing variants reported in the general

660 population are indicated by white circles and white squares, respectively. CADD scores were calculated at

661 http://cadd.gs.washington.edu. WT, wild-type; MAF, minor allele frequency; CADD, combined

662 annotation-dependent depletion; MSC, mutation significance cutoff.

663

664

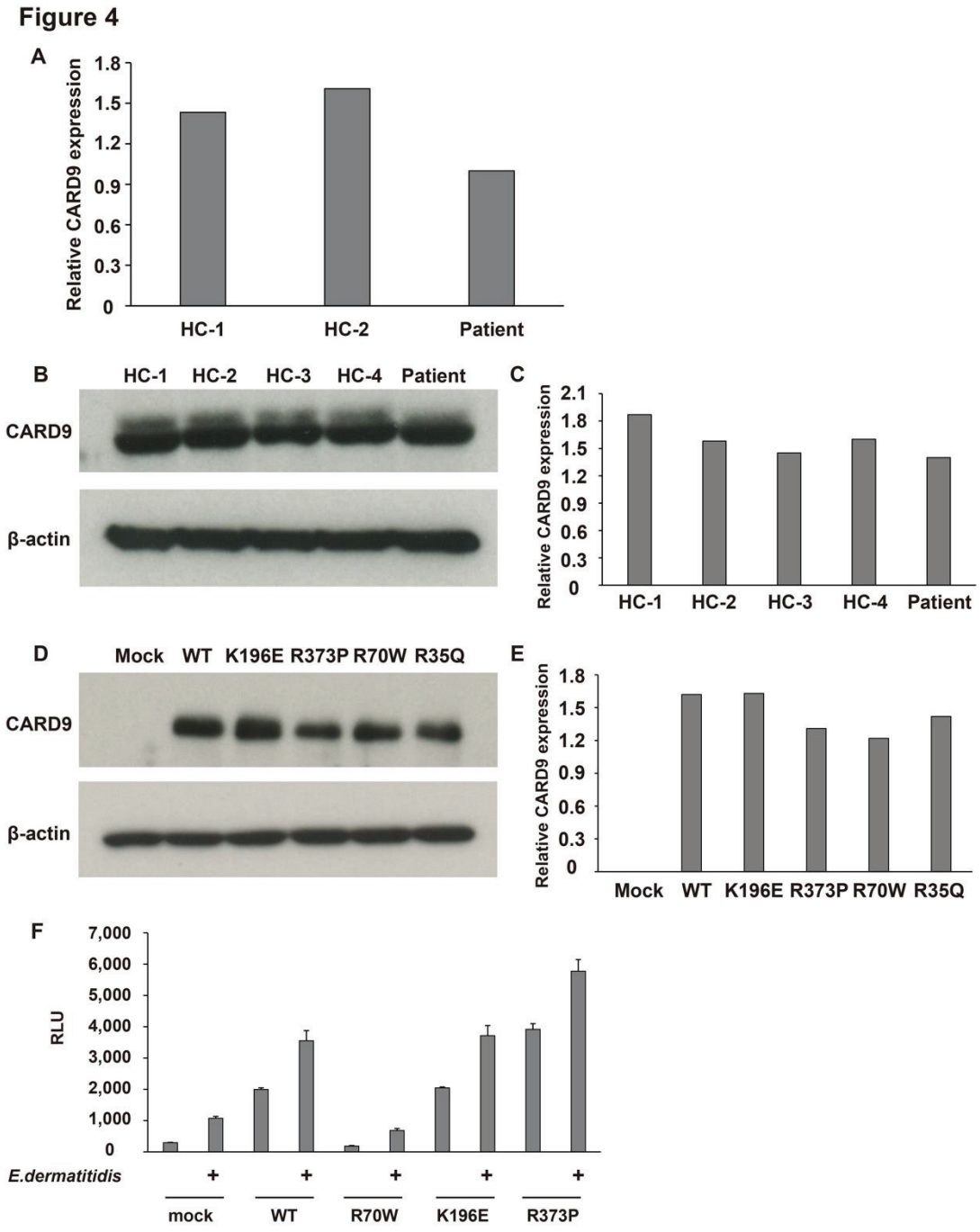

Figure 4

CARD9 mRNA and protein expression and NF-κB transcriptional activity. **A** Relative *CARD9* mRNA expression normalized to *GAPDH* in $CD14^+$ monocytes of the patient and healthy controls (n=2) by quantitative PCR. **B, C** Immunoblot (B) and quantitative analysis (C) of CARD9 expression in $CD14^+$

670 monocytes of the patient and healthy controls (n=4). The results in C show the ratio of CARD9 to β-actin

671 of each individual analyzed. **D**, **E** Immunoblot (D) and quantitative (E) analyses of CARD9 expression in

672 transfected HEK293T cells. The results in E show the ratio of CARD9 to β-actin of each individual analyzed.

673 **F** NF-κB transcriptional activity in transfected HEK293T cells by the NF-κB luciferase assay. HC, healthy

674 control; WT, wild-type; RLU, relative luciferase units.

675

676

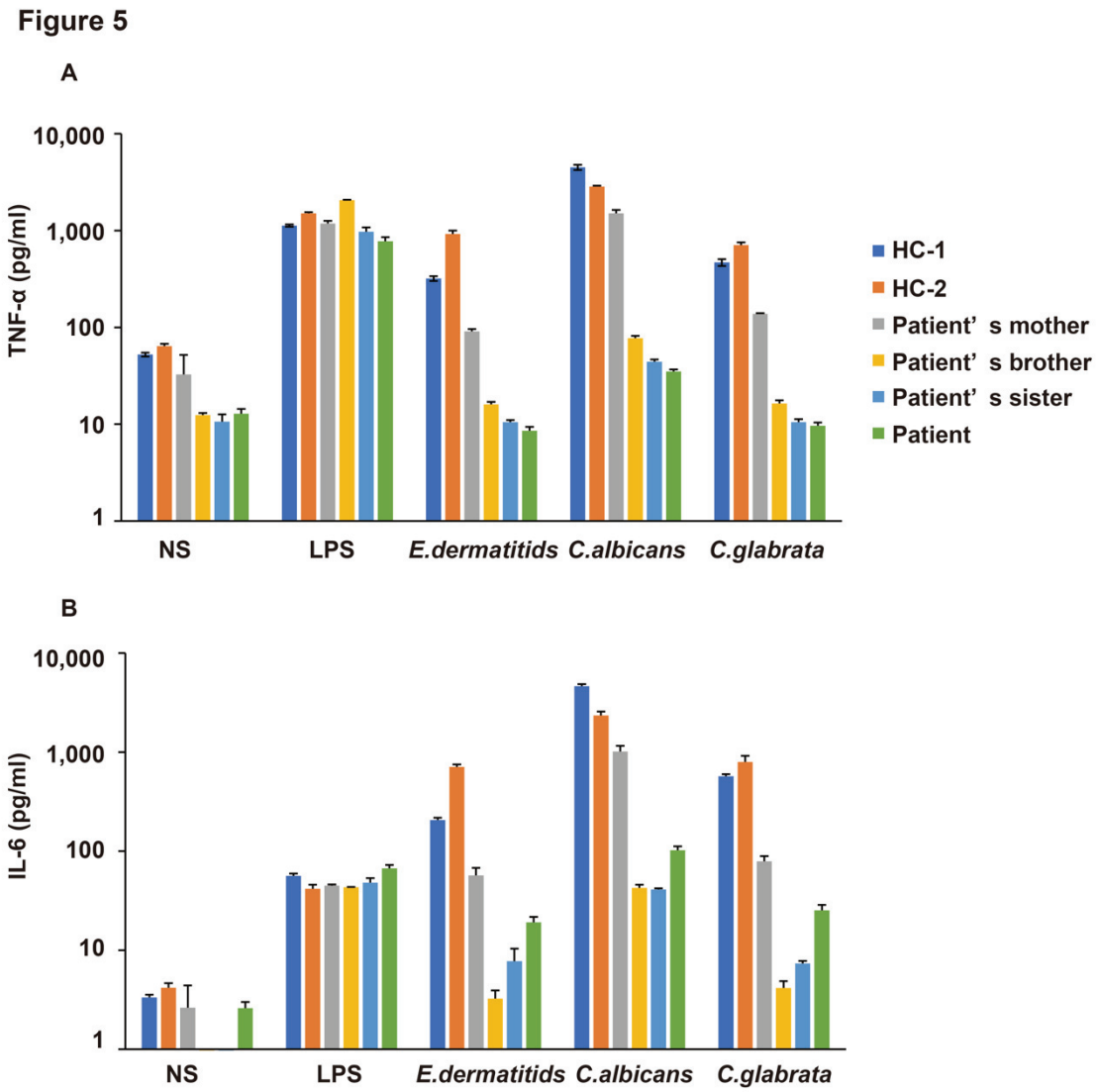

Figure 5

Cytokine production in CD14^{+} monocytes of the patient (p.K196E/p.R373P), the patient's brother (p.K196E/p.R373P), the patient's sister (p.K196E/p.R373P), the patient's mother (p.K196E/WT) and healthy controls (n=2), stimulated with LPS for 2 h or heat-killed *Exophiala dermatitidis*, *Candida albicans,* or *Candida glabrata* for 24 h, as measured by cytometric bead array analysis. **A** TNF-α production. **B** IL-6 production. NS, not stimulated; HC, healthy control

684 **Table S1 Summary of candidate genes by gene panel sequencing**

Gene		dbSNP	ExAC_ALL	gnomAD_ALL	HGVS.c	HGVS.p
AK2	heterozygous	rs202182972	0.005	0.000016	c.614G>A	p.Gly205Glu
BCL11B	heterozygous	.	.	.	c.1151_1152insGTGCATAGGGTTGCC GCGGCCCGGGGACACGGGCCG	p.Arg384_Gly385insCysIleGlyLeu ProArgProGlyAspThrGlyArg
CARD9	heterozygous	rs149712114	0.00004542	0.000022	c.1118G>C	p.Arg373Pro
CARD9	heterozygous	rs768281299	0.00005277	0.000042	c.586A>G	p.Lys196Glu
IL10RA	heterozygous	rs188378450	0.00009914	0.000081	c.313G>A	p.Gly105Ser
IL17RC	heterozygous	rs145374241	0.0001	0.000118	c.655G>A	p.Gly219Ser
IRAK1	heterozygous	.	.	.	c.1453_1466delTGCCCACCTGAGCT insAGCTCAGGTGGGCA	p.CysProProGluLeu485 SerSerGlyGlyGln
KMT2D	heterozygous	.	.	.	c.13885A>C	p.Thr4629Pro
KMT2D	heterozygous	.	.	.	c.5920A>T	p.Thr1974Ser
KMT2D	heterozygous	.	.	.	c.5918_5919insAGCCCG TCCAGGGGCT	p.Trp1973fs
LRBA	heterozygous	.	.	.	c.80C>G	p.Pro27Arg
ORAI1	homozygous	rs141919534	.	.	c.138_143delACCGCC	p.Pro47_Pro48del
PRF1	heterozygous	rs12161733	0.0014	0.000902	c.10C>T	p.Arg4Cys
SH3BP2	heterozygous	rs764213233	0.000009982	0.000013	c.1234C>T	p.His412Tyr
SLC29A3	.	rs2252997	.	.	c.714_715delTGinsCA	p.ThrVal238ThrIle

685 **Table S2 Characteristics of the patient, and her siblings**

	Patient at 4 years old (before treatment)	Patient at 5 years old (after treatment)	Brother at 12 years old	Sister at 11 years old	Normal values
Leukocytes (/ml)	15,540	8,160	5,830	7,270	3,040-8,540
Neutrophils (%)	40.4	35.3	40.2	54.9	38.3-71.1
Eosinophils (%)	26.1	2.5	8.9	1.2	0.2-7.3
Monocytes (%)	3.4	5.4	5.8	4.5	2.7-7.6
Lymphocytes (%)	29.4	56.6	44.6	39.1	21.3-50.2
IgG (mg/dl)	4,254	920	928	972	870-1,700
IgA (mg/dl)	83	42	171	128	110-410
IgM (mg/dl)	163	142	114	118	46-260
IgE (IU/ml)	3.2	NA	339	342	<232
C3 (mg/dl)	150	NA	91	105	86-160
C4 (mg/dl)	33	NA	15	24	17-45
Proliferative response of lymphocytes to PHA (SI)	375	NA	905	500	102-2,644
Proliferative response of lymphocytes to ConA (SI)	192	NA	343	274	74.1-1,793
Leukocyte oxidative burst (DHR)(%)	86.9	NA	86.5	99.3	>80
HIV serology	negative	NA	NA	NA	negative

SI: stimulation index, DHR: dihydrorhodamine, NA: not available

686

687 **Table S3** Lymphocyte subpopulations of the patient, her siblings, and her mother

		Patient at 5 years old	Brother at 12 years old	Sister at 11 years old	Mother at 37 years old	Normal values		
						2-6 years old	7-19 years old	>20 years old
T cells	$CD3^+$/lymphocyte (%)	67.8	68.9	70.1	67.5	69.0 ± 9.0	74.9 ± 12.3	67.8 ± 5.4
	$CD4^+/CD3^+$ (%)	68.8	53.1	56.4	56.1	60.7 ± 7.3	59.4 ± 4.5	59.9 ± 9.9
	$CD45RA^+/CD3^+CD4^+$ (naïve) (%)	85.6	64.1	71.9	35.5	75.9 ± 8.5	65.4 ± 6.0	47.2 ± 9.3
	$CCR7^+CD62\ L^+/CD3^+CD4^+CD45RO^+$ (central memory) (%)	40.2	41.2	49.7	51.3	41.9 ± 11.7	33.0 ± 20.5	30.9 ± 7.9
	$CCR7^-CD62\ L^-/CD3^+CD4^+CD45RO^+$ (effector memory) (%)	14.7	17.2	17.6	18.1	24.0 ± 8.8	27.9 ± 10.3	30.9 ± 7.9
	$CCR6^-CXCR3^+/CD3^+CD4^+CD45RO^+$ (Th1) (%)	22.2	25.9	33.7	22.7	25.0 ± 9.5	23.7 ± 11.1	22.6 ± 8.7
	$CCR6^-CXCR3^-/CD3^+CD4^+CD45RO^+$ (Th2) (%)	60.1	20.9	15.3	13.3	41.4 ± 10.6	40.2 ± 16.5	35.3 ± 13.8
	$CCR6^+CXCR3^-/CD3^+CD4^+CD45RO^+$ (Th17) (%)	13.3	24.6	26.7	41.3	22.2 ± 6.2	25.7 ± 4.7	23.7 ± 4.3
	$IL\text{-}7R^-CD25^+/CD3^+CD4^+\ CCR4^+$ (regulatory T) (%)	2.70	2.60	1.42	2.41	1.65 ± 0.83	2.13 ± 0.60	3.11 ± 1.02
	$CD8^+/CD3^+$ (%)	24.7	35.9	32.9	39.2	29.7 ± 6.7	33.4 ± 9.0	34.1 ± 8.7
B cells	$CD19^+$/lymphocyte (%)	18.2	18.4	17.0	10.2	16.1 ± 7.4	12.4 ± 6.3	12.2 ± 4.4
NK cells	$CD16^+CD56^+$/Lym (%)	1.89	8.56	10.7	13.4	8.8 ± 6.5	7.1 ± 5.8	13.4 ± 4.1

Th: helper T, NK: natural killer

688

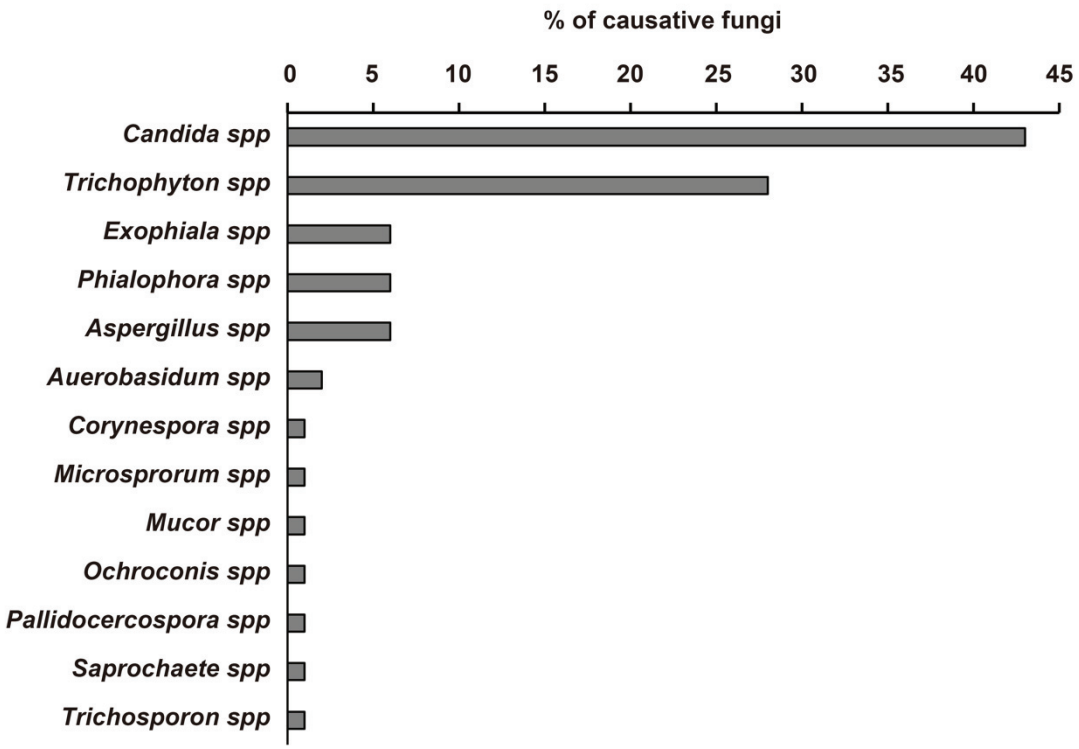

Figure S1

Causative fungi in patients with AR CARD9 deficiency. The percentage of each fungus causing invasive disease in patients with AR CARD9 deficiency is shown.

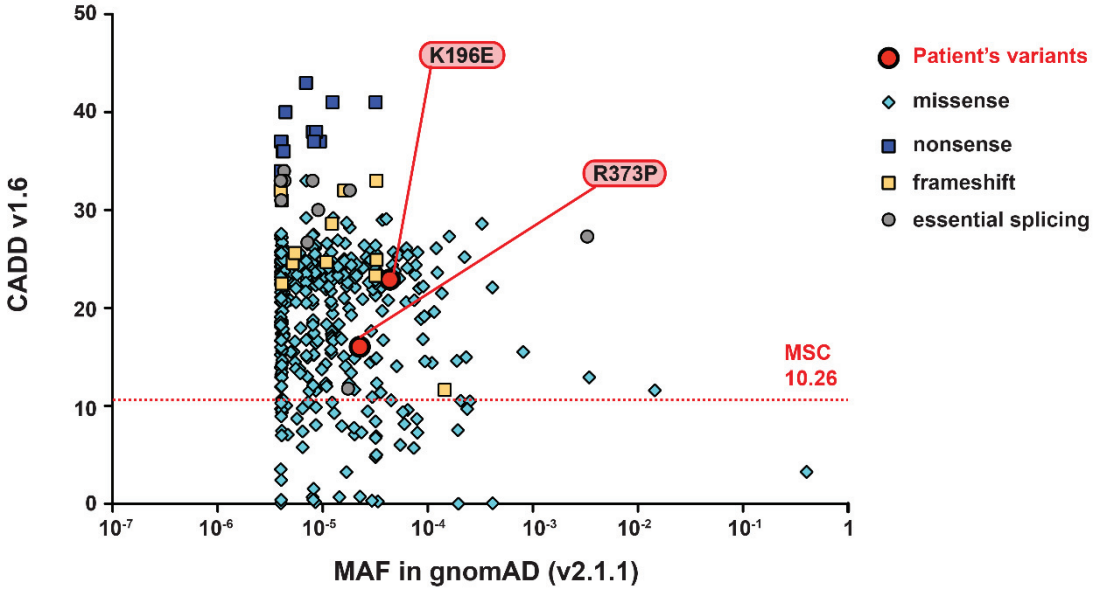

694

695

696 **Figure S2**

697 *In silico* analysis of *CARD9* variants. The graph shows the MAF and CADD v1.6 scores for disease-causing

698 variants identified in our patient and heterozygous variants in the general population, gnomAD v2.1.1

699 (https://gnomad.broadinstitute.org). The red dotted line shows the CADD-MSC score (99% confidence

700 interval) for *CARD9*. The variants identified in our patient are indicated in red circles. Missense, nonsense,

701 frameshift and essential splicing variants in the general population are indicated by light blue diamonds,

702 blue squares, yellow squares, and gray circles, respectively. CADD scores were calculated at

703 http://cadd.gs.washington.edu. MAF, minor allele frequency; CADD, combined annotation-dependent

704 depletion; MSC, mutation significance cutoff.

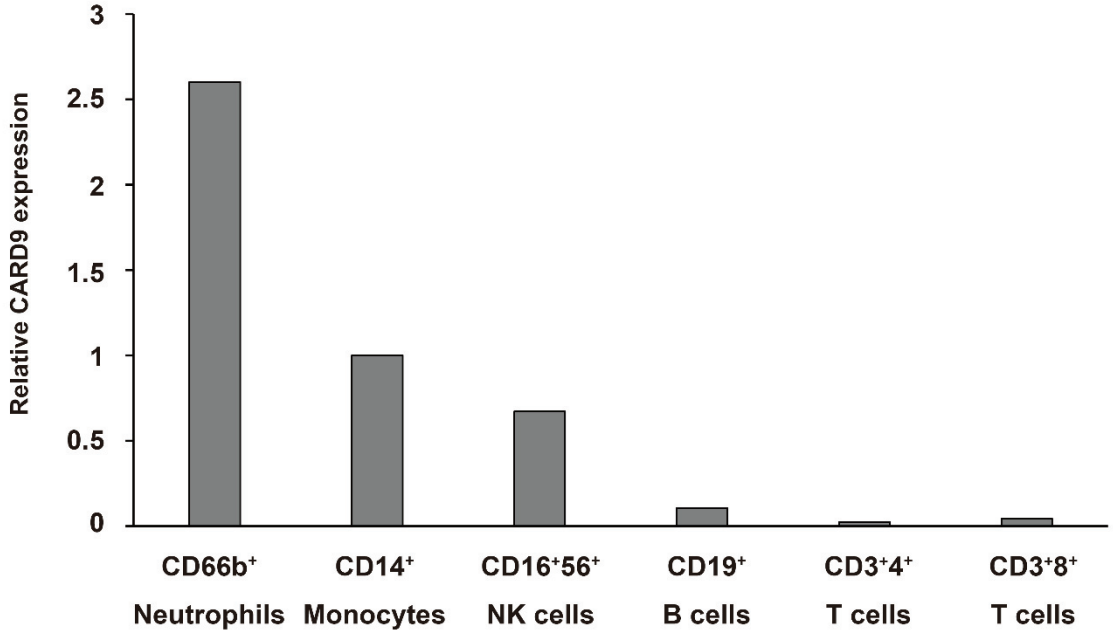

705

706

707 **Figure S3**

708 *CARD9* mRNA expression in peripheral blood subpopulations. Relative *CARD9* mRNA expression

709 normalized to *GAPDH* in $CD66b^+$ neutrophils, $CD14^+$ monocytes, $CD16^+56^+$ NK cells, $CD19^+$ B cells,

710 $CD3^+4^+$ T cells and $CD3^+8^+$ T cells of healthy controls by quantitative PCR.

711

712 **Supplemental materials and methods**

713 **Cell sorting**

714 Peripheral blood cells from healthy donors after the removal of erythrocytes were stained with fluorescently

715 conjugated anti-human CD3, CD4, CD8, CD14, CD16, CD19, CD56, and CD66b (BD Biosciences)

716 antibodies. After surface staining, $CD66b^{+}$ neutrophils, $CD14^{+}$ monocytes, $CD16^{+}56^{+}$ NK cells, $CD19^{+}$ B

717 cells, $CD3^{+}CD4^{+}$ T cells and $CD3^{+}CD8^{+}$ T cells were sorted using a BDFACS Aria™ Cell Sorter (BD

718 Biosciences).

719

720 **Quantitative PCR**

721 Total RNA was extracted from the sorted cells with the Qiagen RNeasy Mini kit (Qiagen) according to the

722 manufacturer's protocol. The detailed method of quantitative PCR is described in the materials and methods.

723